

Reconfigurable quadruple quantum dots in a silicon nanowire transistor

A. C. Betz,^{1,*} M. L. V. Tagliaferri,^{2,3} M. Vinet,⁴ M. Broström,¹
M. Sanquer,⁵ A. J. Ferguson,⁶ and M. F. Gonzalez-Zalba¹

¹Hitachi Cambridge Laboratory, J. J. Thomson Avenue, Cambridge CB3 0HE, United Kingdom

²Laboratorio MDM, CNR-IMM, Via C. Olivetti 2, 20864 Agrate Brianza (MB), Italy

³Dipartimento di Scienza dei Materiali, Universit di Milano-Bicocca, Via Cozzi 53, 20125 Milano, Italy

⁴CEA/LETI-MINATEC, CEA-Grenoble, 17 rue des martyrs, F-38054 Grenoble, France

⁵SPSMS, UMR-E CEA / UJF-Grenoble 1, INAC, 17 rue des Martyrs, 38054 Grenoble, France

⁶Cavendish Laboratory, University of Cambridge, Cambridge CB3 0HE, United Kingdom

(Dated: June 24, 2018)

We present a novel reconfigurable metal-oxide-semiconductor multi-gate transistor that can host a quadruple quantum dot in silicon. The device consist of an industrial quadruple-gate silicon nanowire field-effect transistor. Exploiting the corner effect, we study the versatility of the structure in the single quantum dot and the serial double quantum dot regimes and extract the relevant capacitance parameters. We address the fabrication variability of the quadruple-gate approach which, paired with improved silicon fabrication techniques, makes the corner state quantum dot approach a promising candidate for a scalable quantum information architecture.

Semiconductor quantum bits relying on the charge or spin degree of freedom of a single electron, bound to a quantum dot (QD) or impurity atom, are considered promising candidates for the base elements of solid state quantum computing architectures [1]. Building a successful quantum computer, however, requires a scalable multi-qubit approach to implement the necessary algorithms [2]. Electron spins bound to silicon QDs are seen as promising candidates for this due to their long coherence time, electrical tunability and flexible coupling geometries [3–5]. A further advantage of using Si is the possibility to integrate with current complementary-metal-oxide-semiconductor (CMOS) technology [5–8] and leverage its established industrial platform for large scale circuits. Recently, the integration of Si quantum dots and double quantum dots (DQD) into CMOS technology has been taken a step further with reports of few-electron QDs, DQDs, and donor-QD hybrids created within industry-standard Si nanowire transistors [9–12]. Combined with a gate-based readout scheme that alleviates the need for a separate charge sensor [10–14] these approaches pave the way towards a large scale quantum computing architecture based on current CMOS technology.

In this Letter, we report on a reconfigurable QD and DQD system in a quadruple-gate CMOS transistor. It incorporates one, or a pair, of CMOS corner state quantum dots [10, 11] in a variety of configurations. Each of the four gates can host an independently tunable quantum dot created in the square channel by electrostatic enhancement and confinement resulting from the top-gate electrodes and accompanying silicon nitride spacers. We characterise one exemplary single QD and demonstrate that different DQD configurations can be set at will. Building on previous demonstrations [10–12], our

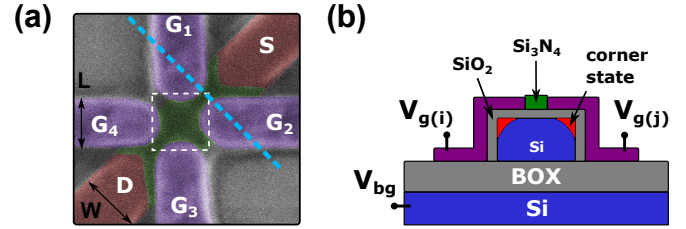


FIG. 1: Device geometry (a) Top-view scanning electron micrograph of the device. The Si_3N_4 region is highlighted in green, highly doped leads are red, and gate electrodes are coloured purple. (b) Sketch of device cross-section perpendicular to transport direction. A corner state quantum dot can be created under each gate at the top-most corners of the channel (see (a)). Each QD is controlled by its respective gate voltage $V_{g(x)}$, while a global backgate voltage V_{bg} may be applied through the Si substrate.

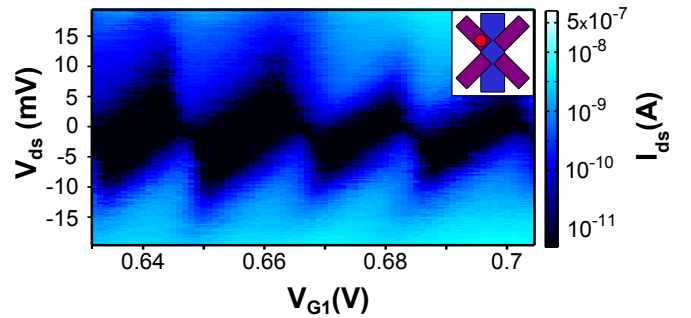


FIG. 2: Charge stability diagram of quantum dot under gate G_1 at $V_{g4} = 1.4$ V, and $V_{g2} = V_{g3} = 0$ V.

results provide a way to scale up CMOS quantum information architectures and to create reconfigurable silicon multi-dot arrangements.

The device presented here is a fully depleted silicon-on-insulator (FDSOI) nanowire field-effect transistor with four independently addressable top-gates. The poly-

*Electronic address: ab2106@cam.ac.uk

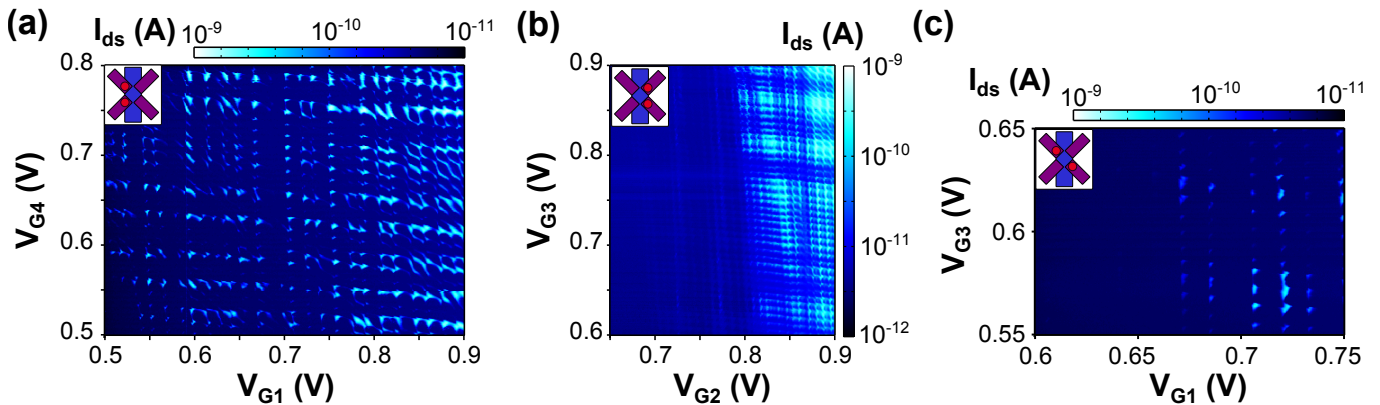


FIG. 3: Different DQD configurations established in the FDSOI nanowire transistor. Serial DQD created along gates (a) G_1 - G_4 , (b) G_2 - G_3 , and (c) G_1 - G_3 .

silicon top-gates of length $L = 40$ nm are arranged around the sides of a $82 \text{ nm} \times 82 \text{ nm}$ square at 45° with respect to transport direction as shown in white dashes in the scanning electron micrograph of a similar device in Fig.1(a). Gate-to-gate distances are $S_{G_1-G_2} = S_{G_2-G_3} = 30$ nm, and the channel width W is 87 nm. Fig.1(a) shows the Si_3N_4 spacers deposited between the gates and extending 40 nm towards source and drain in green. The channel below remains undoped generating the source, drain and inter-dot tunnel barriers. Fig.1(b) shows a cross-section sketch of the device perpendicular to the direction of transport, taken at the line indicated by the cyan line in Fig.1(a). The device comprises an Si back plane serving as global backgate, topped by a 150 nm SiO_2 buried oxide. This is followed by the undoped, square Si (001) channel of thickness 12 nm, which is achieved by etching down the SOI substrate prior to gate stack deposition. Each top-gate wraps around two faces of the intrinsic channel and is separated from the other top-gates by the Si_3N_4 spacers and from the channel by 5 nm of SiO_2 [15]. A quantum dot can be created under each gate at the top-most corners of the channel due to the so-called corner effect [10, 11, 16]. Each QD is controlled by its respective gate voltage $V_{g(x)}$, while a global backgate voltage V_{bg} may be applied through the Si substrate. All measurements shown in this Letter are in direct transport and unless otherwise stated were taken at $V_{bg} = 5$ V, to enhance the dot-to-dot and dot-to-lead couplings [17].

Corner state quantum dots in Si nanowire transistors have been reported for different single and double gate topologies [9–11] and using both quantum dots and dopants [12]. In our novel quadruple gate configuration, we first of all confirm the creation of a single QD under a top-gate using gate G_1 as an example. In order to allow for a source-drain current, G_4 is pulled high above threshold to $V_{g_4} = 1.4$ V, while the gates on the opposite channel side remain well below threshold at $V_{g_2} = V_{g_3} = 0$ V. The backgate voltage is set to 0 V. This provides a single QD under gate G_1 , as can be seen from the stability map

of Fig.2. We extract a charging energy $E_{c,G_1} \simeq 9$ meV and source and drain capacitances $C_{s,G_1} \simeq 2$ aF and $C_{d,G_1} \simeq 1$ aF from the slope of the Coulomb diamonds and the gate voltage period. Single QDs embedded in a multi-gate structure like the one investigated here could host single electron spin qubits, or be used as single-electron transistors for charge detection of a nearby dot.

The ability to create multi-QD configurations is, as mentioned above, an important ingredient in the pursuit of a scalable semiconductor QIP architecture. In the following paragraphs we demonstrate that different configuration of serial DQDs can be formed in the nanowire transistor and extract the DQD coupling capacitances. All following measurements were carried out at a small source-drain voltage $V_{ds} = 2$ mV. First of all, we configure the device as a serial DQD on the G_1 - G_4 axis, by setting $V_{g_2} = V_{g_3} = 0$ V. Fig.3(a) shows the resulting DC current I_{ds} as a function of V_{g_1} and V_{g_4} . In the stability map, we observe a honeycomb pattern and at its vertices we find the so-called bias triangles, i.e. periodic regions of enhanced current resulting from the alignment of both QD energy levels within the bias window, indicative of a serial DQD [18]. At low voltages on both G_1 and G_4 the stability map shows the checker box behaviour characteristic for low inter-dot coupling, transitioning to the aforementioned honeycomb arrangement for intermediate coupling strength. At elevated top-gate voltages the inter-dot coupling increases, resulting in undulated diagonal lines of enhanced conductance indicating that the QDs are strongly tunnel coupled [19]. The voltage spacing of Coulomb oscillations in the low to intermediate coupling regime is $\Delta V_{g_1} \simeq 11$ mV and $\Delta V_{g_4} \simeq 14$ mV (see also Fig.4(a)). Both spacings are very regular across the voltage range studied here, indicating stable QD position and size. Fig.3(b) presents the opposite configuration to Fig.3(a), a serial DQD along G_2 - G_3 with now $V_{g_1} = V_{g_4} = 0$ V. Similarly to Fig.3(a) we obtain a honeycomb diagram, albeit a more compressed one with $\Delta V_{g_2} \simeq 9$ mV and $\Delta V_{g_3} \simeq 8$ mV, indicating larger QDs. Finally, Fig.3(c) shows the stability map for a diago-

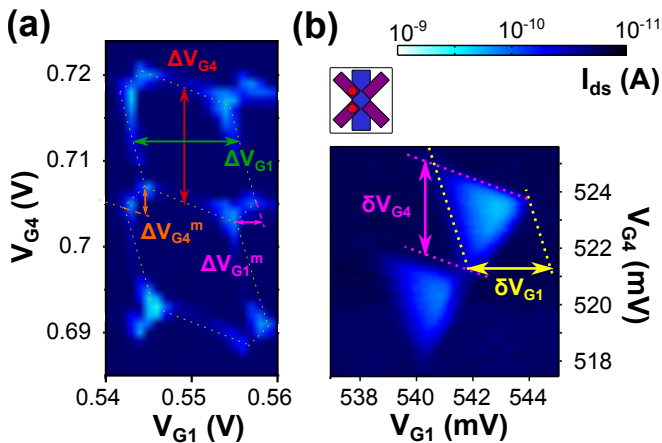


FIG. 4: Zoom of G_1 - G_4 honeycomb diagram. (a) Honeycomb diagram along several bias triangles, outlined by yellow dashed lines. (b) Bias triangles at voltages below (a).

nal DQD using G_1 and G_3 as constituent quantum dots. Here, the overall current is reduced compared to the previous two configurations, which we attribute to the larger distance between the dots under G_2 and G_3 and hence reduced inter-dot tunnel rates. We extract Coulomb spacings $\Delta V_{g1} \simeq 13$ mV and $\Delta V_{g3} \simeq 7$ mV, approximately in line with the previous results. Similar results have been obtained for the DQD along the G_2 - G_4 axis (not shown here).

Last but not least, we study the serial DQD along G_1 - G_4 in more detail to obtain estimates of the capacitances involved in the system. From the honeycomb diagram outlined in Fig.4(a) we extract voltage spacings $\Delta V_{G1} \simeq 11$ mV and $\Delta V_{G4} \simeq 14$ mV between Coulomb oscillations. These spacings are linked to the gate capacitances of the two serial QDs as $\Delta V_{Gi} = e/C_{Gi}$ [18] and we thus estimate $C_{G1} \simeq 15$ aF and $C_{G4} \simeq 12$ aF. Applying this analysis to the G_2 - G_3 configuration, we find gate capacitances $C_{G2} \simeq 12$ aF and $C_{G3} \simeq 20$ aF. The voltage spacings δV_{G1} and δV_{G4} extracted from Fig.4(b) in combination with the source-drain voltage $V_{sd} = 2$ mV provide us with an estimate for the lever arms $\alpha_{1(4)}$ and total capacitances $C_{1(4)}$ as $\alpha_{1(4)}\delta V_{G1(4)} = e|V_{sd}| = e\delta V_{G1(4)}C_{G1(4)}/C_{1(4)}$ [18]. We find lever arms $\alpha_{1(4)} \simeq 0.55$ (0.49) and total capacitances $C_{1(4)} \simeq 26$ (23) aF. These values in addition to $\Delta V_{g1(4)}^m$ from Fig.4(a) allow us now to also approximate the mu-

tual capacitance linking the QDs under gates G_1 and G_4 : $C_{m,1-4} = C_4\Delta V_{g1}^m/\Delta V_{g1} \simeq 6$ aF. The same analysis carried out for the diagonal DQD along G_1 - G_3 (not shown here) yields a mutual capacitance $C_{m,1-3} \simeq 4$ aF.

Variability between nominally identical devices from different batches but also within a single batch fabricated at the same time is an important benchmarking parameter in CMOS technology. Comparing all four gate capacitances of the device presented here, we find a mean gate capacitance of about 16 aF and a variance of 25%. We attribute this variance to variations in gate dielectric thickness and quality, as well as gate misalignment relative to the channel. All three factors directly influence the enhancement mode corner state QDs.

In conclusion, we have demonstrated a reconfigurable quantum dot and double quantum dot system based on a quadruple-gate CMOS transistor. Taking into account the continuous improvement of CMOS fabrication techniques and the single electron control demonstrated here, corner state quantum dots present a valid and scalable option as base elements of a silicon quantum information architecture. Moreover, this approach can readily be extended to a larger number of gates providing a 1-D line of QDs and DQDs, while remaining compact by further integrating high-sensitivity gate-based reflectometry readout [10, 11]. The versatility of the corner state QD structure allows to use the gate-based sensing either for in-situ readout, but also for conventional charge sensing using an rf-single electron box for detection. Further experiments that can be envisioned with this architecture are e.g. electron charge and electron spin buses, measurements of long distance coherent coupling [20], and single spin CCD [21].

The authors thank D.A. Williams and M. Fanciulli for support and discussion. The research leading to these results has been supported by the European Community's seventh Framework under the Grant Agreement No. 214989. The samples presented in this work were designed and fabricated by the AFSID project partners (www.afsid.eu). A.J. Ferguson acknowledges support from EPSRC (EP/K027018/1) and from his Hitachi research fellowship. M.L.V. Tagliaferri acknowledges support from the Short Term Mobility Program 2015 of Consiglio Nazionale delle Ricerche (CNR), Italy.

-
- [1] F. A. Zwanenburg, A. S. Dzurak, A. Morello, M. Y. Simmons, L. C. L. Hollenberg, G. Klimeck, S. Rogge, S. N. Coppersmith, and M. A. Eriksson, *Rev. Mod. Phys.* **85**, 961 (2013).
 [2] D. P. DiVincenzo, *Fortschritte Der Physik* **48**, 771 (2000).
 [3] M. Veldhorst, J. C. C. Hwang, C. H. Yang, A. W. Leenstra, B. de Ronde, J. P. Dehollan, J. T. Muhonen,

- F. Hudson, K. M. Itoh, A. Morello, and A. S. Dzurak, *Nat. Nano.*, 981 (2014).
 [4] D. Kim, Z. Shi, D. R. Simmons, C. B. and Ward, J. R. Prance, T. S. Koh, J. K. Gamble, D. E. Savage, M. G. Lagally, M. Friesen, S. N. Coppersmith, and M. A. Eriksson, *Nature* **511**, 70 (2014).
 [5] M. Veldhorst, C. H. Yang, J. C. C. Hwang, W. Huang, J. P. Dehollan, S. Muhonen, J. T. and Simmons,

- A. Laucht, F. Hudson, K. M. Itoh, A. Morello, and A. S. Dzurak, *Nature* **526**, 410 (2015).
- [6] S. J. Angus, A. J. Ferguson, A. S. Dzurak, and R. G. Clark, *Nano Letters* **7**, 2051 (2007).
- [7] J. J. Pla, K. Y. Tan, J. P. Dehollain, W. H. Lim, J. J. L. Morton, F. A. Zwanenburg, D. N. Jamieson, A. S. Dzurak, and A. Morello, *Nature* **496**, 334 (2013).
- [8] A. Crippa, M. L. V. Tagliaferri, D. Rotta, M. De Michielis, G. Mazzeo, M. Fanciulli, R. Wacquez, M. Vinet, and P. E., *Physical Review B* **92**, 035424 (2015).
- [9] B. Voisin, V.-H. Nguyen, J. Renard, X. Jehl, S. Barraud, F. Triozon, M. Vinet, I. Duchemin, Y.-M. Niquet, S. de Franceschi, and M. Sanquer, *Nano Letters* **14**, 2094 (2014).
- [10] A. C. Betz, R. Wacquez, M. Vinet, X. Jehl, A. L. Saraiva, M. Sanquer, A. J. Ferguson, and M. F. Gonzalez-Zalba, *Nano Letters* **15**, 4622 (2015).
- [11] M. F. Gonzalez-Zalba, S. Barraud, A. J. Ferguson, and A. C. Betz, *Nature Communications* **6** (2015), doi:10.1038/ncomms7084.
- [12] M. Urdampilleta, A. Chatterjee, C. C. Lo, T. Kobayashi, J. Mansir, S. Barraud, A. C. Betz, S. Rogge, M. F. Gonzalez-Zalba, and J. J. L. Morton, *Phys. Rev. X* **5**, 031024 (2015).
- [13] J. I. Colless, A. C. Mahoney, J. M. Hornibrook, A. C. Doherty, H. Lu, A. C. Gossard, and D. J. Reilly, *Physical Review Letters* **110**, 046805 (2013).
- [14] M. F. Gonzalez-Zalba, S. N. Shevchenko, S. Barraud, J. R. Johansson, A. J. Ferguson, F. Nori, and A. C. Betz, *Nano Letters* **0**, null (2016), pMID: 26866446, <http://dx.doi.org/10.1021/acs.nanolett.5b04356>.
- [15] M. Hofheinz, X. Jehl, M. Sanquer, G. Molas, M. Vinet, and S. Deleonibus, *Applied Physics Letters* **89** (2006), <http://dx.doi.org/10.1063/1.2358812>.
- [16] H. Sellier, G. P. Lansbergen, J. Caro, S. Rogge, N. Collaert, I. Ferain, M. Jurczak, and S. Biesemans, *Applied Physics Letters* **90** (2007).
- [17] B. Roche, B. Voisin, X. Jehl, R. Wacquez, M. Sanquer, M. Vinet, V. Deshpande, and B. Prevtali, *Applied Physics Letters* **100**, 032107 (2012), <http://dx.doi.org/10.1063/1.3678042>.
- [18] W. G. van der Wiel, S. De Franceschi, J. M. Elzerman, T. Fujisawa, S. Tarucha, and L. P. Kouwenhoven, *Reviews of Modern Physics*, **75**, 1 (2002).
- [19] N. S. Lai, W. H. Lim, C. H. Yang, F. A. Zwanenburg, W. A. Coish, F. Qassemi, A. Morello, and A. S. Dzurak, *Scientific Reports* **1** (2011), 10.1038/srep00110.
- [20] F. R. Braakman, P. Barthelemy, C. Reichl, W. Wegscheider, and L. M. K. Vandersypen, *Nature Nanotechnology* **8**, 432 (2013).
- [21] T. Baart, M. Shafiei, T. Fujita, C. Reichl, W. Wegscheider, and L. M. K. Vandersypen, *Nature Nanotechnology* (2015), 10.1038/nnano.2015.291.